Journal of Power Sources 196 (2011) 2759–2762

Contents lists available at ScienceDirect

Journal of Power Sources

journal homepage: www.elsevier.com/locate/jpowsour

Short communication

Behaviors of proton exchange membrane fuel cells under oxidant starvation

Meiling Dou[a,b], Ming Hou[a,*], Dong Liang[a,b], Qiang Shen[a,b], Huabing Zhang[a,b], Wangting Lu[a,b], Zhigang Shao[a,**], Baolian Yi[a]

[a] Fuel Cell system and engineering laboratory, Dalian Institute of Chemical Physics, Chinese Academy of Sciences, Dalian 116023, China
[b] Graduate University of Chinese Academy of Sciences, Beijing 100049, China

ARTICLE INFO

Article history:
Received 3 September 2010
Received in revised form 2 November 2010
Accepted 3 November 2010
Available online 10 November 2010

Keywords:
Proton exchange membrane fuel cell (PEMFC)
Oxidant starvation
Current distribution
Local interfacial potential

ABSTRACT

Durability is an important issue in proton exchange membrane fuel cells (PEMFCs) currently. Reactant starvation could be one of the reasons for PEMFC degradation. In this research, the oxidant starvation phenomena in a single cell are investigated. The local interfacial potential, current and temperature distribution are detected in situ with a specially constructed segmented cell. Experimental results show that during the cell reversal process due to oxidant starvation, the local interfacial potential in the oxidant inlet keeps positive while that of the middle and outlet regions become negative, which illustrates that oxygen and proton reduction reactions could occur simultaneously in different regions at the cathode. The current distribution would be more uneven with decreasing air stoichiometry before cell reversal. When cell reversal occurs, the current will redistribute and the current distribution tends more uniform. At the critical point of cell reversal, the most significant inhomogeneity in the current distribution can be observed. The temperature distribution in the cell is also monitored on-line. The local hot spot exists in the cell when cell reversal occurs. The study of the critical reversal air stoichiometry under different loads shows that the critical reversal air stoichiometry increases with the rising loads.

1. Introduction

Durability appears to be one of the barriers of PEMFC commercialization [1–3]. Oxidant starvation, usually occurring under harsh operating conditions such as sub-zero start-up, rapid load change and water accumulation during long-term operation, etc. [4,5], is one of the potential factors to result in the degradation of PEMFCs. In a fuel cell stack, if the oxygen supplied is not enough to maintain the stack current, the oxidant starvation will occur. In this case, a reversal of cell voltage could happen. In the absence of oxygen, protons pass through the membrane and combine with each other. Thus hydrogen is produced to provide the compensatory current [6,7]. The oxidant starvation behavior of fuel cell has been studied by some researchers [7–10]. Taniguchi et al. [10] investigated the changes of cell voltage, electrode potentials against RHE with time during oxidant starvation and found the inhomogeneous degradation of catalyst. Liu et al. [7] analyzed the current distribution during oxidant starvation and observed the decreased local current density in the starvation region.

In our previous paper [11], the reversal processes of a single cell under fuel starvation conditions were well discussed. In this work, we utilized the current distribution measurement system and the local interfacial potential method to fulfill a comprehensive understanding of the reversal process during oxidant starvation. Current, potential and temperature distribution under different air stoichiometries were detected in situ. The experimental results of this paper could supply some useful information for durability researches on fuel cell vehicles (FCVs).

2. Experimental

A segmented cell including a specially designed MEA and a cathode end plate was constructed to measure the current distribution and the local electrode potentials. The MEA with a total active area of 230.36 cm^2 consisted of Nafion® 212 membranes as the electrolyte, catalyst layers with the total Pt loading of 0.8 mg cm^{-2} and Toray paper as diffusion layers. A short stack was electrically connected with the segmented cell to provide power for the single cell reversal. The detailed description could be found in our previous paper [11].

In this experiment, the hydrogen and air were humidified using spraying method. The temperature of the fuel cell was kept at 60 °C. The reaction gases were both under saturated humidification and kept at ambient pressure, operating in the co-flow mode. The hydrogen stoichiometry was fixed at 2.0 and the air stoichiometry was varied. The compositions and contents of the exhaust gas at the cathode were analyzed in situ by gas phase chromatogram (SHI-

* Corresponding author. Tel.: +86 411 84379051; fax: +86 411 84379185.
** Corresponding author. Tel.: +86 411 84379153; fax: +86 411 84379185.
E-mail addresses: houming@dicp.ac.cn (M. Hou), zhgshao@dicp.ac.cn (Z. Shao).

0378-7753/$ – see front matter © 2010 Elsevier B.V. All rights reserved.
doi:10.1016/j.jpowsour.2010.11.005

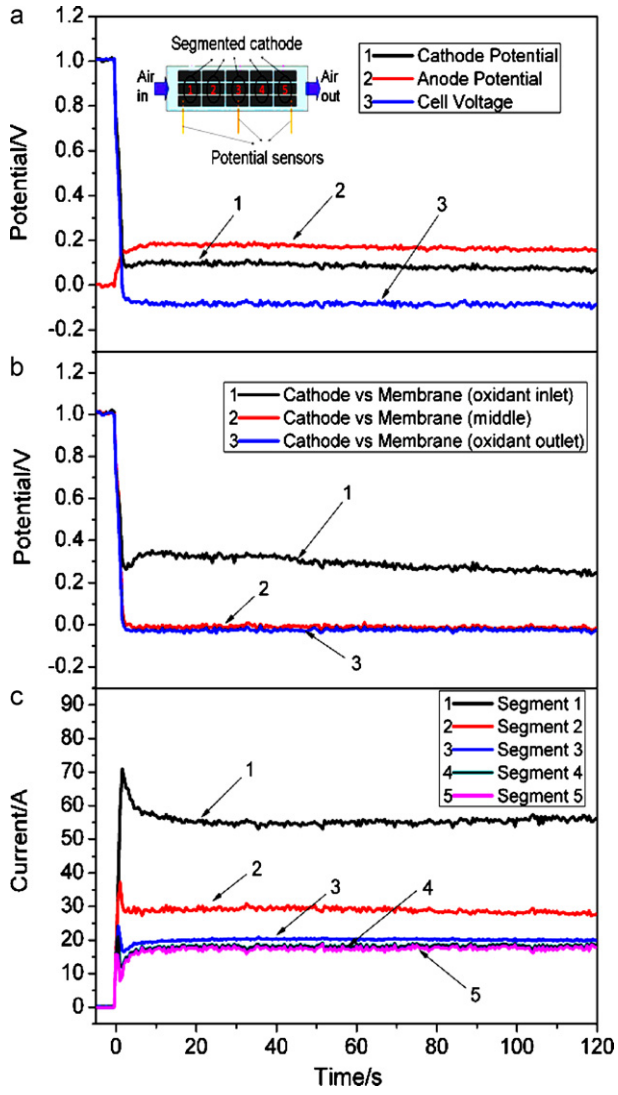

Fig. 1. The changes of (a) cell voltage and electrode potentials, (b) local interfacial potentials between cathode and membrane, and (c) current distribution with time under the air stoichiometry of 0.9 (load 600 mA cm^{-2}).

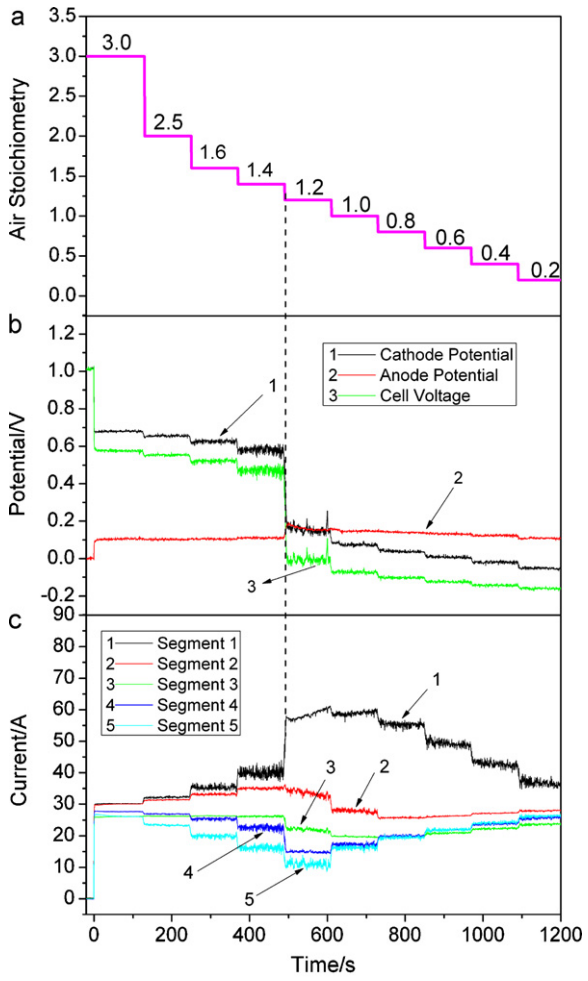

Fig. 2. The changes of (a) the set values of air stoichiometries, (b) the cell voltage and electrode potentials, and (c) the current distribution with time under different air stoichiometries from 3.0 to 0.2 (load 600 mA cm^{-2}).

MADAZU GC-14C). Three mini-size thermocouples, made of copper and constantan thermocouple wires with diameter of 80 μm, were embedded between the MEA and the cathode flow field at the inlet, middle and outlet separately, to measure the temperature inside the fuel cell. The mini-size thermocouples were all calibrated before the experiments.

3. Results and discussion

3.1. Tests under oxidant starvation condition

Fig. 1 depicts the response characteristics of PEMFC under oxidant starvation condition (air stoichiometry 0.9). Fig. 1(a) shows the changes of cell voltage and electrode potentials with time under oxidant starvation conditions. It is observed that the cathode potential suddenly drops due to lack of oxygen and the cell voltage decreases to ca. −0.08 V, implying that the cell reversal occurs. However, unlike the deep cell reversal (cell voltage below −1.0 V) observed in the case of fuel starvation [11], oxidant starvation induces a low magnitude cell reversal. Fig. 1(b) shows the response of the local interfacial potentials between cathode and membrane with time along the cathode channels. It can be seen that the local interfacial potentials at the middle and outlet of the cathode both decrease to negative promptly, while the local interfacial potential at cathode inlet still keeps positive although it also decreases significantly. This indicates that the proton reduction reaction could take place near the cathode middle and outlet, and the reaction at the cathode inlet is still oxygen reduction under the air stoichiometry of 0.9. The current distribution as shown in Fig. 1(c) exhibits significant variation across the cell plane. The current of segment 1 increases to 55 A dramatically, largely higher than those of segments 3–5 (all below 30 A). The local current decreases from gas inlet to outlet, which suggests that oxygen is consumed gradually along the flow direction.

3.2. The influence of air stoichiometry

Fig. 2 illustrates the dependence of cell voltage, electrode potentials and current distribution on the variation of air stoichiometry under the load of 600 mA cm^{-2}. It can be seen that the cathode potential and cell voltage reduce with the decrease of air stoichiometry. As the air stoichiometry decreases to 1.2, the cell voltage drops to 0 V sharply, which indicates that the air stoichiometry of 1.2 is the critical point of cell reversal at the current density of 600 mA cm^{-2}.

The distribution of current along the cathode channels as shown in Fig. 2(c) is extremely sensitive to air stoichiometry. When the air stoichiometry changes from 3.0 to 1.2, the current near the inlet of the cathode increases, while that of region near the outlet

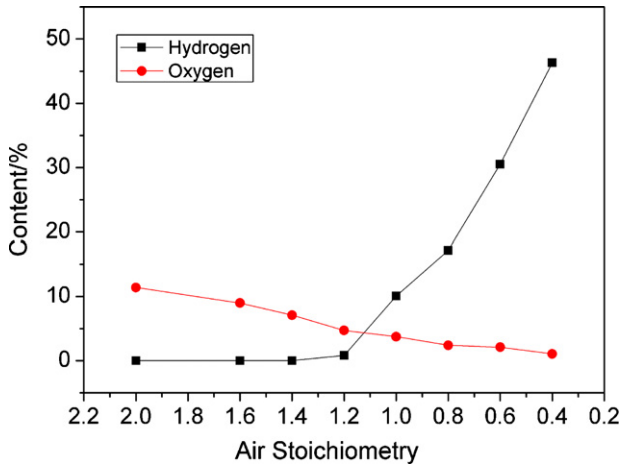

Fig. 3. The contents of hydrogen and oxygen in cathode exhaust gas under different air stoichiometries.

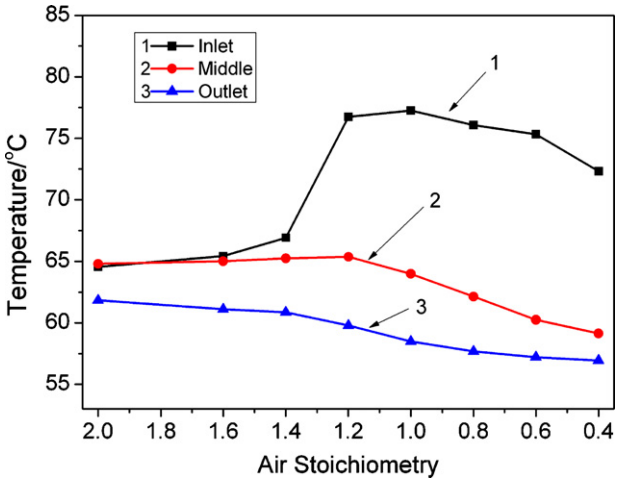

Fig. 4. The changes of temperature under different air stoichiometries (the average value during the last 30 s).

decreases. As a result, the current distribution tends to be more heterogeneous. The reason for this is that the local current distribution along the cathode channels is mainly dominated by the gradient of oxygen concentration. Near the cathode inlet the oxygen concentration is the highest, the local current density is the greatest. As oxygen is consumed along the cathode channels, the oxygen concentration decreases down the flow direction, resulting in a drop in current density in segments downstream. With the air stoichiometry decreasing, the gradient of oxygen concentration increases, which results in more inhomogeneous current distribution. When the air stoichiometry decreases to 1.2, the current at the inlet rises sharply and the current distribution is extremely heterogenous.

In a contrast, when the air stoichiometry decreases from 1.2 to 0.2, the current distribution tends to be more homogeneous, which indicates that the current would redistribute during the process of oxidant starvation. The result shows that the decrease of air stoichiometry reduces the current of the inlet (oxygen reduction current) and correspondingly increases that of the outlet (proton reduction current). It is likely because that the local current distribution along the cathode channels is mainly influenced by the proton reduction reaction. The lower the air stoichiometry is, the higher the proportion of the proton reduction current is. This could be proved by the compositions and contents of the cathode exhaust gas under different air stoichiometries shown in Fig. 3. As indicated in Fig. 3, under the oxidant starvation conditions, with the decrease of air stoichiometry, the content of the oxygen decreases while that of hydrogen increases, indicating higher proportion of the proton reduction reaction. The results above indicate that the proportion of proton reduction current to the overall current increases as the decrease of air stoichiometry, and the oxidant starvation would become more severe. As a result, the current distribution in fuel cell turns to be more uniform.

Fig. 4 shows the temperature along the cathode channels inside the cell under different air stoichiometries. Before cell reversal (air stoichiometry 2.0–1.4), the temperature of cathode inlet increases while that of the outlet reduces with the decreasing air stoichiometry. The difference between the inlet and outlet is less than 6 °C. At the point of cell reversal (air stoichiometry is 1.2), the temperature of cathode inlet increases to 77 °C dramatically while that of cathode outlet is lower than 60 °C. After cell reversal (air stoichiometry 1.2–0.4), the temperatures of both cathode inlet and outlet decrease with the decreasing air stoichiometry. However, the temperature of the cathode inlet is largely higher than that of the outlet. The temperature difference between the inlet and outlet reaches as large as 19 °C. Such heterogenous temperature distribution may be relative to the uneven current distribution shown in Fig. 2(c). Furthermore, the proton reduction reaction taken place near the cathode outlet may also lead to the decrease of the temperature. The results above show that the oxidant starvation can result in the local hot spot in the cell, which is likely to cause the local degradation of the MEA. Thus the membrane degradation may occur due to the high temperature during the cell reversal process. Moreover, the cathode catalyst may be damaged with the production of hydrogen, such as platinum dissolution. However, the low cathode potential experienced would not induce some significant corrosion of the cathode support.

3.3. The influence of current density

Fig. 5 shows the cell voltage changes with air stoichiometries (varied from 1.5 to 1.0) under different loads. If the oxidant is not enough to maintain the stack current, the proton reduction may take place near the cathode outlet to provide the current, which will make the voltage of the starved cells drop to negative. Then there must be a point of air stoichiometry at which the cell reversal just happens. Here, we define the point as “critical reversal air stoichiometry”. As shown in Fig. 5, when the loads are set at 500 mA cm^{-2}, 600 mA cm^{-2}, 700 mA cm^{-2} and 800 mA cm^{-2}, the critical reversal air stoichiometries are 1.1, 1.2, 1.3 and 1.4, respectively. The results indicate that the larger the working current density is, the higher the critical reversal air stoichiometry is. Fur-

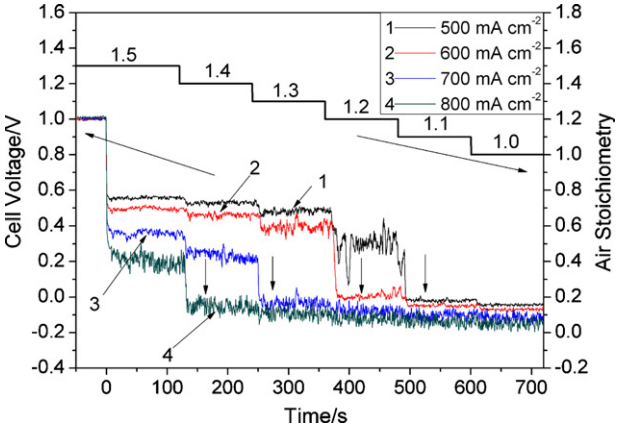

Fig. 5. The changes of the cell voltage with air stoichiometries (varied from 1.5 to 1.0) under different loads.

thermore, the critical reversal air stoichiometry against the load appears to be linear, which agrees well with Fick's first law. The reason for this is that oxygen concentration in the catalyst layer is too low to sustain the needed current, thus cell reversal happens. The higher the working current density of the cell is, the higher the oxygen concentration is needed. Therefore, the critical reversal air stoichiometry increases with the rising working current density, which is attributed to the higher driving force needed for the mass transfer at higher current density. As a result, in order to minimize the mass transfer resistance, the electrode and other structure parameters of the fuel cell should be optimized as much as possible.

4. Conclusions

In this work, the behaviors of a unit cell in a PEMFC stack under oxidant starvation conditions have been explored. Experimental results show that when oxidant starvation occurs, the current distribution is uneven, and the local interfacial potentials between cathode and membrane in different regions differ significantly. Oxygen and proton reduction reactions could occur simultaneously in different regions at the cathode. The current distribution results show that the most significant difference exists in the current distribution at the critical point of cell reversal. With the air stoichiometry decreasing, the current distribution is more heterogeneous before cell reversal, while after cell reversal the corresponding current distribution tends to be more uniform. With the increasing degree of oxidant starvation, the proportion of proton reduction current to the total current rises. The study of the critical reversal air stoichiometry under different loads shows that the critical reversal air stoichiometry increases with the rising load. Unlike fuel starvation, oxidant starvation has little influence on carbon corrosion (no high potential). The local hot spots have been observed at the cathode air inlet. That would be a possible reason for the degradation of the MEA. Future efforts should include the degradation mechanism exploration of fuel cells under oxidant starvation.

Acknowledgments

This work was financially supported by the National Natural Science Foundations of China (nos. 20876155, 20936008).

References

[1] N. Yousfi-Steiner, P. Mocotéguy, D. Candusso, D. Hissel, J. Power Sources 194 (2009) 130–145.
[2] Q. Yan, H. Toghiani, H. Causey, J. Power Sources 161 (2006) 492–502.
[3] J. Xie, D.L. Wood III, D.M. Wayne, T.A. Zawodzinski, P. Atanassov, R.L. Borup, J. Electrochem. Soc. 152 (2005) A104–A113.
[4] M.A. Danzer, S.J. Wittmann, E.P. Hofer, J. Power Sources 190 (2009) 86–91.
[5] X. Yan, M. Hou, L. Sun, H. Cheng, Y. Hong, D. Liang, Q. Shen, P. Ming, B. Yi, J. Power Sources 163 (2007) 966–970.
[6] S.D. Knights, K.M. Colbow, J. St-Pierre, D.P. Wilkinson, J. Power Sources 127 (2004) 127–134.
[7] Z. Liu, L. Yang, Z. Mao, W. Zhuge, Y. Zhang, L. Wang, J. Power Sources 157 (2006) 166–176.
[8] K. Mitsuda, T. Murahashi, J. Appl. Electrochem. 21 (1991) 524–530.
[9] R.H. Song, C.S. Kim, D.R. Shin, J. Power Sources 86 (2000) 289–293.
[10] A. Taniguchi, T. Akita, K. Yasuda, Y. Miyazaki, Int. J. Hydrogen Energy 33 (2008) 2323–2329.
[11] D. Liang, Q. Shen, M. Hou, Z. Shao, B. Yi, J. Power Sources 194 (2009) 847–853.